(0.047 g, 47%) as viscous yellow oils.

X-ray Crystal Structure Analysis of 2. $C_{14}H_{10}O_4Fe$, M = 298.1, monoclinic, space group $P2_1/c$, a = 13.998 (6) Å, b = 7.955 (5) Å, c = 12.935 (5) Å, β = 113.04 (3)°, U = 1325 (1) Å^3, Z = 4, D_c = 1.49 g cm^{-1}. Data were collected with a Syntex $P2_1$ four-circle diffractometer, maximum 2θ 50°, using Mo Kα radiation, λ = 0.71069 Å, μ(MoKα) = 11.4 cm^{-1}, T = 293 K, crystal dimensions 0.12 × 0.30 × 0.64 mm. Profile analysis gave 2343 unique reflections (R_{int} = 0.03); 1854 were considered observed [$I/\sigma(I) > 2.0$] and used in refinement; they were corrected for Lorentz, polarization, and absorption effects, the last by the Gaussian method. The Fe atom was located from a Patterson synthesis, and the light atoms were then found on successive syntheses (including H atoms). Anisotropic temperature factors were used for all non-H atoms. Hydrogen atoms were given fixed isotropic temperature factors. Phenyl H atoms were inserted at calculated positions and not refined; the methyl group was treated as a rigid CH_3 unit, with its original orientation taken from the strongest H-atom peaks on a difference Fourier synthesis. Other H-atom coordinates were refined. Final refinement was on F by cascaded least-squares methods refining 181 parameters. A weighting scheme of the form $w = 1/[\sigma^2(F) + gF^2]$ with g = 0.0014 was used and shown to be satisfactory by a weight analysis: final R = 0.039, R_w = 0.043; maximum shift/error in final cycle 0.03. Computing was with SHELXTL (Sheldrick, 1983) on a Data General DG30. Scattering factors in the analytical form and anomalous dispersion factors were taken from *International Tables* (1974).

Acknowledgment. We thank Dr. O. W. Howarth and Dr. J. Lall for ^{13}C NMR spectra and Mr. I. K. Kaytal for mass spectra data. We also acknowledge financial support from the S.E.R.C.

Supplementary Material Available: Listings of thermal parameters, bond lengths and angles, and H atom coordinates (3 pages); a table of observed and calculated structure factors (14 pages). Ordering information is given on any current masthead page.

Rigid Bent Bridges between Cyclopentadienylmetal Fragments. Iron Derivatives of the 4,8-Ethano-2,4,6,8-tetrahydro-*s*-indacene-2,6-diyl Dianion†

Hermann Atzkern, Brigitte Huber, Frank H. Köhler,* Gerhard Müller,‡ and Reinhard Müller

Anorganisch-chemisches Institut, Technische Universität München, D-8046 Garching, FRG

Received April 20, 1990

From the reaction of the 4,8-ethano-2,4,6,8-tetrahydro-*s*-indacene-2,6-diyl dianion (L) and cyclopentadienyl (Cp) anion with iron(II) chloride the bridged ferrocenes *syn,syn*-CpFeLFeCp (**4**), *syn,anti*-CpFeLFeCp (**5**), and *all-syn*-CpFeLFeLFeCp (**6**) were obtained. The structures of **4–6**, including syn, anti isomerism, were deduced from their ^1H and ^{13}C NMR and mass spectra. X-ray crystal analyses were carried out for **4** and **5** (**4**, monoclinic, $P2_1/n$, a = 8.665 (1) Å, b = 7.724 (1) Å, c = 26.286 (2) Å, β = 97.82 (1)°, R_w = 0.028 for 235 refined parameters and 3107 observables; **5**·0.5C_6H_6, monoclinic, $P2_1/n$, a = 6.087 (1) Å, b = 41.475 (4) Å, c = 7.995 (1) Å, β = 96.58 (1)°, R_w = 0.074 for 262 refined parameters and 2219 observables). They showed that both molecules are rather distorted, leading to Fe–Fe distances which are almost 0.5 Å longer than those expected for an idealized geometry. In the cyclic voltammograms of **4–6** separate waves indicated that the ferrocene units were oxidized at different potentials. These potentials were shown to depend on the number of bridges and $CpFe^+$ fragments next to the ferrocene unit under study. The separation of the potentials reflected the metal–metal interaction.

Introduction

Bridging of ligands is a general strategy for assembling two or more metal fragments in close proximity. The resulting compounds are expected to have properties that differ from those of the mononuclear analogues, owing to extended interactions between the metals. One possibility for tailoring these interactions is precise stereochemical control by the ligand. For the cyclopentadienyl (Cp) anion various linear arrangements of type A have been realized.[1]

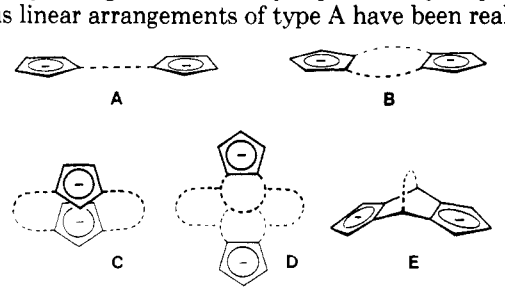

Scheme I

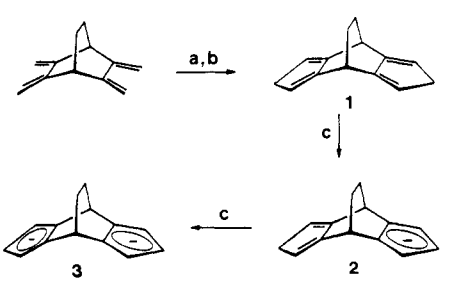

[a] t-BuOK/$CHBr_3$. [b] (1) MeLi, (2) H_2O. [c] MeLi.

However, for A the orientation of the π-systems relative to each other is difficult to adjust. A better approach are cofacial and the noncofacial stacks obtainable from type C[2] or type D[3] ligands or the coplanar arrangement B.[4]

† Dedicated to Professor I. Ugi on the occasion of his 60th birthday.

‡ Present address: Fakultät für Chemie, Universität Konstanz, D-7750, Konstanz, FRG.

(1) (a) Müller-Westerhoff, U. T. *Angew. Chem.* **1986**, *98*, 700; *Angew. Chem., Int. Ed. Engl.* **1986**, *25*, 702. (b) Bunel, E. E.; Campos, P.; Ruz, J.; Valle, L.; Chadwick, I.; Santa Ana, M.; Gonzalez, G.; Manriquez, J. M. *Organometallics* **1988**, *7*, 474. (c) Bunel, E. E.; Valle, L.; Jones, N. L.; Carroll, P. J.; Gonzalez, M.; Munoz, N.; Manriquez, J. M. *Organometallics* **1988**, *7*, 789.

0276-7333/91/2310-0238$02.50/0

Scheme II

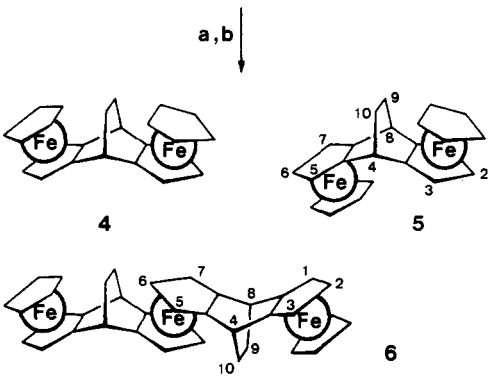

[a] CpNa. [b] 3.

When the angular dependence of interfragment interactions is to be exploited, the potential of A–D is rather limited. In particular, no general access to Cp–metal compounds was known in which an interplanar angle exists between the π-systems as represented in E. We have recently bridged two Cp anions by bicyclo[2.2.2]octane and -octene,[5] thus arriving at an angle of approximately 120°. Here we examine the potential binding of these ligands to transition metals, the precise stereochemistry, and the metal–metal interaction, choosing 4,8-ethano-2,4,6,8-tetrahydro-*s*-indacene and iron(II) as an example.

Results and Discussion

Synthesis. The title ligand **1** has been obtained in good yield from 2,3,5,6-tetramethylenebicyclo[2.2.2]octane as shown in Scheme I. Its deprotonation, which was most conveniently effected with methyl- or *n*-butyllithium, did not give the expected dianion **3** directly. Thus, when 1 equiv of MeLi was added to a solution of **1** in THF/TMEDA (6/1), the ^{13}C NMR spectrum showed signals that are typical for a 1,2-disubstituted Cp anion (δ 97.34, 96.11, and 122.46; intensities approximately 1/2/2) and a 1,2-disubstituted cyclopentadiene (δ 40.46, 112.65, and 155.33; intensities 1/2 and a smaller signal for quaternary carbon atoms). These two sets of signals, which are different from those of **1** and **3**, were good evidence that the monoanion **2** had been formed. Addition of an excess of MeLi gave **3** quantitatively (^{13}C NMR).

The most simple metallocenes derived from **3** should be **4** and **5**, shown in Scheme II. Since the reaction of a mixture of Cp^- and **3** with solvated iron(II) chloride was expected to yield considerable amounts of oligomers and ferrocene, the reaction was carried out stepwise. Thus, at −78 °C step a in Scheme II gave a green mixture, which pointed to the formation of a cyclopentadienyliron chloride species. Without isolation this was further reacted with **3** (step b). Workup gave an orange-red material, from which some ferrocene was removed by sublimation. Chromatography of the remainder gave three main fractions, from which ferrocene, the syn,syn isomer **4**, and the syn,anti isomer **5** could be isolated in good yield (34.7 and 27.5% for **4** and **5**, respectively relative to **1**). However, the yield of ferrocene (29.5% relative to Cp^-) indicated that the reaction is not very selective. This is in accord with earlier attempts to synthesize $(C_5Me_5)FeCp$.[6] A fourth small fraction resulting from chromatography gave the trinuclear compound **6**.

Mass Spectroscopy. The mass spectra of **4**–**6** established the number of iron atoms and of Cp and bridging ligands per molecule. For all compounds the molecular ion was the base peak and the experimental isotope pattern (mass 420–424 for **4** and **5** and mass 656–661 for **6**) was in good agreement with the calculated intensities. After determination of the stereochemistry by NMR spectroscopy and X-ray crystallography an interesting dependence of the fragmentation on the molecular structures became apparent. The molecular ion of the syn,anti isomer **5** (base peak) easily lost the ethano bridge, giving $M^+ - C_2H_4$ with 69% relative intensity and an experimental isotope pattern that is somewhat distorted probably due to loss of hydrogen. For the syn,syn isomer **4** $M^+ - C_2H_4$ was found with only 3% intensity. Two reasons may be responsible for this. (i) $M^+ - C_2H_4$ has the two CpFe units trans to each other when derived from **5** and cis when derived from **4**. For steric reasons $4^+ - C_2H_4$ should therefore be less stable than $5^+ - C_2H_4$. (ii) The ethano bridge is split off easily only if it is not buried by two CpFe units as in **4**. The relative intensity of $M^+ - C_2H_4$ (or $M^+ - C_{2n}H_{4n}$ for oligonuclear compounds) may therefore be used tentatively to determine the stereochemistry of similar molecules. In fact, when this method was applied to **6**, a 2% peak for $M^+ - C_2H_4$ and a 0.2% peak for $M^+ - 2C_2H_4$ suggested an all-syn arrangement, which was proven independently by NMR spectroscopy.

NMR Studies. The ^1H and ^{13}C NMR signals of **4**–**6** were found in shift ranges that are well-known for the nuclei of ferrocenes or those in bridgehead (such as 4,8) and bridge (such as 9,10) positions. Therefore, in the case of **4**, with a high local symmetry of the bridging ligand, the interpretation of the spectra is straightforward (Table I). An accidental coincidence of the signals of C1,3,5,7 and C2,6 was found in benzene. This was verified by selective decoupling: irradiation at H2,6 gave a singlet for C2,6 and a residual doublet for C1,3,5,7, both centered at 62.29 ppm. A useful feature is the high-frequency signal shift of H9,10 when passing from **1** (δ 1.73) to **4** (δ 2.61). The shift is due to the fact that, according to the X-ray results below, H9,10 lie well in the deshielding zone defined for sandwich molecules.[7] This shift allows an unequivocal decision whether a CpFe unit is arranged syn or anti with respect to the ethano bridge in less symmetric molecules. For instance, two signals at 2.29 and 1.47 ppm with a geminal coupling of 6.6 Hz were found for H9,10 of **5**. This established the syn,anti isomer, which was confirmed independently by X-ray crystallography. A second example is **6**, where the number of ^{13}C NMR signals was consistent with three isomers: the syn,syn,syn,syn, the anti,syn,-

(2) (a) Arnold, R.; Foxman, B. M.; Rosenblum, M. *Organometallics* **1988**, *7*, 1253. (b) Jutzi, P.; Siemeling, U.; Müller, A.; Bögge, H. *Organometallics* **1989**, *8*, 1744.

(3) Hopf, H.; Dannheim, J. *Angew. Chem.* **1988**, *100*, 724; *Angew. Chem., Int. Ed. Engl.* **1988**, *27*, 701.

(4) (a) Hafner, K. *Angew. Chem.* **1963**, *75*, 1041. (b) Katz, T. J.; Schulman, J. *J. Am. Chem. Soc.* **1964**, *86*, 3169. (c) Miyake, A.; Kanai, A. *Angew. Chem.* **1971**, *83*, 851; *Angew. Chem., Int. Ed. Engl.* **1971**, *10*, 801. (d) Katz, T. J.; Acton, N.; McGinnis, J. *J. Am. Chem. Soc.* **1972**, *94*, 6205. (e) Katz, T. J.; Slusarek, W. *J. Am. Chem. Soc.* **1979**, *101*, 4259. (f) Katz, T. J.; Slusarek, W. *J. Am. Chem. Soc.* **1980**, *102*, 1058. (g) Edlund, U.; Eliasson, B.; Kowalewski, J.; Trogen, L. *J. Chem. Soc., Perkin Trans. 2* **1981**, 1260. (h) Stezowski, J. J.; Hoier, H.; Wilhelm, D.; Clark, T.; Schleyer, P. v. R. *J. Chem. Soc., Chem. Commun.* **1985**, 1263. (i) Sudhakar, A.; Katz, T. J. *J. Am. Chem. Soc.* **1986**, *108*, 179. (j) Bell, W. L.; Curtis, C. J.; Eigenbrot, C. W., Jr.; Pierpont, C. G.; Robbins, J. L.; Smart, J. C. *Organometallics* **1987**, *6*, 266.

(5) Atzkern, H.; Köhler, F. H.; Müller, R. *Z. Naturforsch., B: Anorg. Chem., Org. Chem.* **1990**, *45*, 329.

(6) Kölle, U.; Fuss, B.; Khouzami, F.; Gersdorf, J. *J. Organomet. Chem.* **1985**, *290*, 77.

(7) Elschenbroich, C.; Schneider, J.; Prinzbach, H.; Fessner, W.-D. *Organometallics* **1986**, *5*, 2091.

Table I. ^{13}C and ^{1}H NMR Data[a] for 4–6

position of nuclei[b]	compd 4	compd 5	compd 6
1,3	62.29 d, *173.6*[c] 3.74 d, *2.2*	62.37[f,g] d, *174.1*[h] 3.88[f] d, *2.2*	62.30 d, *174.1* 3.73[g] d, *2.2*
5,7	62.29 d, *173.6*[c] 3.74 d, *2.2*	62.66[f,g] d, *173.6*[i] 4.01 d, *2.2*	62.30 d, *164.1* 3.79[g] d, *2.2*
2	62.29 d[d] 3.56 t, *2.2*	64.26[f] d, *158.5*[c] 3.76[g] t, *2.2*	64.12 d, *166* 3.58[f,g] t, *2.2*
6	62.29 d[d] 3.56 t, *2.2*	61.89 d, *159.4*[c] 3.75[g] t, *2.2*	64.12 d, *166* 3.67[f,g] t, *2.2*
3a,8a	100.85 s	99.33[f] s	100.74[f,g] s
4a,7a	100.85 s	94.61 s	100.27[f,g] s
4,8	32.45 d, *139.9* 3.24 t, *1.5*	32.70 d, *140.4* 3.35[j]	32.52 d, *139.8* 3.31[j]
9,10	33.64 t, *131.3* 2.61 t, *1.4*	32.25 t, *132.8* 2.29[k] d, *6.6* 1.47[l] d, *6.6*	33.42 2.60[j,m]
syn-Cp	68.94 d, *174.6*[e] 4.03 s	69.05[f,g] d, *175.3*[e] 3.99[f] s	68.99 d, *174.6*[e] 4.06 s
anti-Cp		68.85[f,g] d, *174.4*[e] 3.83 s	

[a] Obtained in C_6D_6 at 310 K. Entries give $\delta(^{13}C)$, the multiplicity due to directly bound protons, and $^{1}J(CH)$ (Hz) in italics in the first line for each nucleus and $\delta(^{1}H)$, multiplicity, and $J(HH)$ (Hz) in italics in the second line. [b] For the numbering see Scheme II. [c] Additional splitting $^{2}J(CH) \approx {}^{3}J(CH) = 6.7$ Hz (t). [d] Obscured by C1,3,5,7. [e] Additional splitting into virtual quintets: $J(CH) = 6.7$ Hz. [f] Assignment proposed after comparison with **4** or **6**. [g] Interchange of the assignment to 1,3 or 5,7, 2 or 6, 3a,8a or 4a,7a, and *syn*-Cp or *anti*-Cp not excluded. [h] Additional splitting: $^{2}J(CH \approx {}^{3}J(CH) = 6.6$ Hz (t), $^{3}J(CH) = 2.0$ Hz (d). [i] Additional splitting: $^{2}J(CH) \approx {}^{3}J(CH) = 6.4$ Hz (t), $^{3}J(CH) = 2.6$ Hz (d). [j] Broadened by unresolved couplings. [k] Syn. [l] Anti. [m] Syn and anti not resolved.

Table II. Selected Distances (Å) and Angles (deg) for 4 with Esd's in Units of the Last Significant Figure in Parentheses[a]

Fe–D1	1.66	Fe–D4	1.66
Fe–D2	1.66	Fe–D3	1.67
Fe1···Fe2	6.11		
C1–C2	1.518 (3)	C1–C6	1.525 (3)
C3–C4	1.519 (3)	C4–C5	1.515 (3)
C2–C3	1.419 (3)	C5–C6	1.423 (3)
C2–C9	1.421 (3)	C6–C14	1.425 (3)
C3–C11	1.425 (3)	C5–C12	1.423 (3)
C9–C10	1.436 (4)	C13–C14	1.431 (3)
C10–C11	1.429 (4)	C12–C13	1.434 (4)
C1–C7	1.544 (3)	C4–C8	1.551 (3)
C7–C8	1.548 (3)		
C2–C1–C6	102.4 (2)	C3–C4–C5	102.3 (2)
C2–C1–C7	107.4 (2)	C3–C4–C8	107.6 (2)
C6–C1–C7	107.3 (2)	C5–C4–C8	107.1 (2)
C1–C7–C8	110.7 (2)	C4–C8–C7	111.4 (2)
C1–C2–C3	114.1 (2)	C1–C6–C5	114.2 (2)
C2–C3–C4	114.2 (2)	C4–C5–C6	113.8 (2)

[a] D1–D4 denote the centroids of the Cp rings; see Figures 1 and 2.

syn,anti, and the syn,anti,anti,syn isomer. Since for H9,10 only one broad signal appeared at 2.60 ppm, **6** must be the all-syn isomer. Obviously the central and the outer ferrocene moieties are not sufficiently different to give an observable splitting of this signal at 270 MHz.

Solid-State Structures of 4 and 5. Besides the dinuclear syn,syn and syn,anti isomers **4** and **5**, one may also think of an anti,anti isomer. Simple models of **3** (e.g. in Scheme I) show, however, that there is not enough space at the two π-faces below the ethano bridge to accommodate two CpM fragments in a η^5-bonding fashion. In order to probe the structural particularity of the bridging ligand, which may also have an influence on the metal–metal

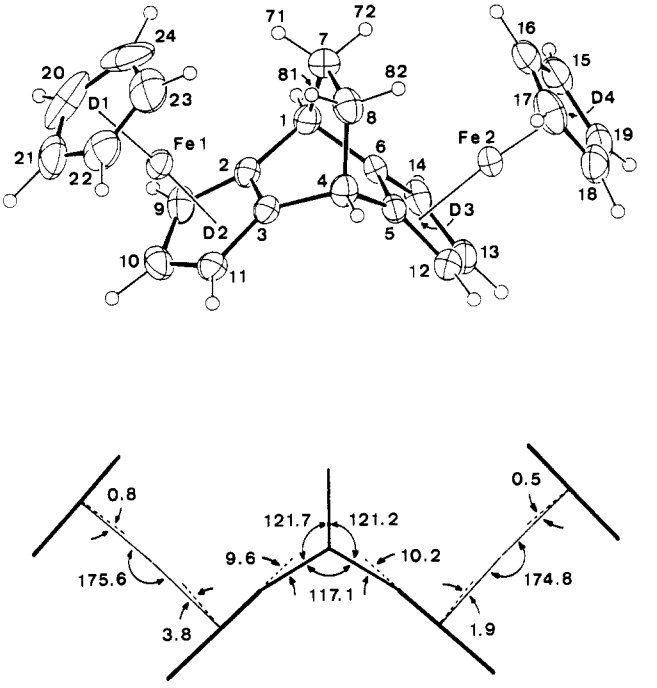

Figure 1. (Top) Molecular structure of **4** and atomic numbering used (Tables II and VI; ORTEP, displacement ellipsoids at the 50% probability level, H atoms with arbitrary radii). (Bottom) Selected interplanar angles (deg).

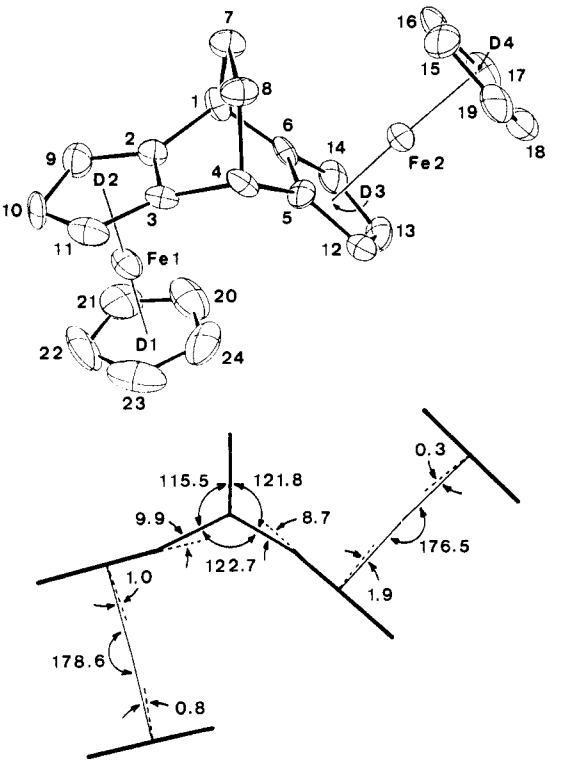

Figure 2. (Top) Molecular structure of **5** and atomic numbering used (Tables III and VII). The H atoms were omitted, because they were much less defined than in **4**. (Bottom) Selected interplanar angles (deg).

interaction, X-ray structure analyses were carried out for **4** and **5**.

The molecular structures of **4** and **5** are shown in Figures 1 and 2, and selected bond lengths and angles are given in Tables II and III. Two ferrocene units are linked by the central bicyclic moiety such that both are syn relative to the ethano bridge in **4** or syn and anti in **5**. Both

Table III. Selected Distances (Å) and Angles (deg) for 5

Fe1-D1	1.66	Fe2-D4	1.68
Fe1-D2	1.65	Fe2-D3	1.67
Fe1···Fe2	5.34		
C1-C2	1.49 (1)	C1-C6	1.47 (1)
C3-C4	1.52 (1)	C4-C5	1.51 (1)
C2-C3	1.43 (1)	C5-C6	1.43 (1)
C2-C9	1.43 (1)	C6-C14	1.44 (1)
C3-C11	1.39 (1)	C5-C12	1.43 (1)
C9-C10	1.46 (1)	C13-C14	1.43 (2)
C10-C11	1.40 (1)	C12-C13	1.42 (1)
C1-C7	1.57 (1)	C4-C8	1.53 (1)
C7-C8	1.60 (1)		
C2-C1-C6	107.8 (9)	C3-C4-C5	105.6 (8)
C2-C1-C7	104.5 (8)	C3-C4-C8	102.7 (8)
C6-C1-C7	108.5 (8)	C5-C4-C8	108.3 (8)
C1-C7-C8	108.2 (8)	C4-C8-C7	111.2 (8)
C1-C2-C3	113.9 (9)	C1-C6-C5	113.2 (9)
C2-C3-C4	113.5 (9)	C4-C5-C6	114.8 (9)

Table IV. Cyclic Voltammetric Data[a] for 4-6

	compd and solvent				
	4, THF	5, THF	6, THF	4, PrCN	5, PrCN
$E_{1/2}(1)$	400	410	300	330	350
$\Delta E_p(1)$	100	110	70	85	110
$E_{1/2}(2)$	560	550	490	530	545
$\Delta E_p(2)$	80	90	70	90	80
$E_{1/2}(3)$			590		
$\Delta E_p(3)$			70		
$\Delta E_{1/2}(2-1)$	160	140	190	200	195
$\Delta E_{1/2}(3-2)$			100		

[a] In mV. Conditions for THF solvent: potential vs SCE, 25 °C, scan rate 50 mV s^{-1}. Conditions for PrCN solvent: potential vs Ag/AgCl/3 M KCl, 25 °C, scan rate 200 mV s^{-1}. Consecutive oxidations are given in parentheses with the CV symbols.

molecules have been designed as rigid dinuclear metallocenes, and yet they depart considerably from idealized geometry. For instance, the neighboring planes of the ferrocenes and the bicyclic moiety are not coplanar. As shown in the lower part of Figures 1 and 2, the average fold angle about the fusing edges C2–C3 and C5–C6 is 9.6°. All five-membered rings are bent away from the ethano bridge, except when the ferrocene is in the anti position. This is equivalent to a bending of the metallocene substituents away from the metal.

In most of the metallocenes Cp_2M the hydrogen atoms are bent toward the metal,[8] which has been explained by orbital overlap effects.[9] In contrast, substituents are bent away from the metal because the transannular steric effect overrides the electronic effect. In the case of **4** and **5** the corresponding angle[10] is about 4 times bigger than in $(C_5Me_5)_2Fe$.[11] Hence, in **4** and **5** the steric repulsion between the ethano bridge and *syn*-CpFe or the second ferrocene unit and *anti*-CpFe is more important than the transannular effect.

There are other distortions that have the same steric origin. For instance, the Cp ligands of the ferrocene units are not parallel. They include angles of up to 9°, which are composed of the metallocene bending angles and the angles between the vectors Fe–D (D = center of Cp) and the normals to the Cp planes given in Figures 1 and 2.

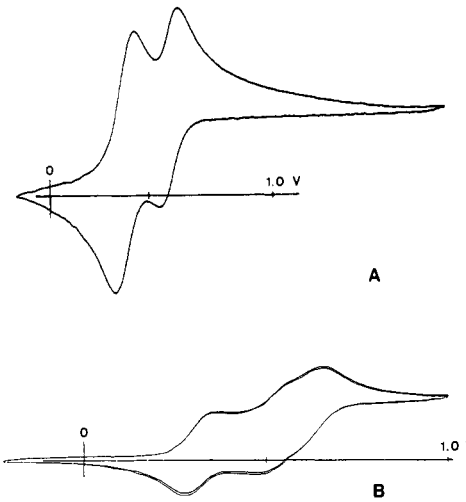

Figure 3. Cyclic voltammograms of **4** in propionitrile vs Ag/AgCl/3 M KCl, with scan rate 200 mV s^{-1} (A), and of **6** in THF vs SCE, with scan rate 50 mV s^{-1} (B).

Another distortion is observed for the bicyclic bridges. Their interplane angles open to >120° whenever a CpFe unit fills the gap.

For other fused ligands similar distortions have been found. Examples are the CpCo(diene)-type molecules **7**

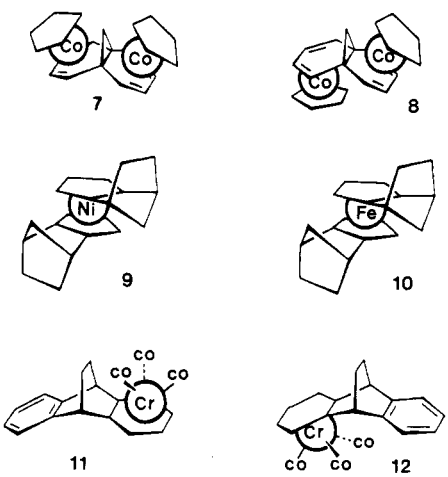

and **8**,[12] which are further related to **4** and **5** because they exist as syn,syn and syn,anti isomers. The structures of the metallocenes **9**[13] and **10**[14] have also been reported. They are mononuclear but resemble **4** and **5** in that a bicyclic moiety is fused to the π-ligand. A similar reasoning applies for the $(CO)_3Cr$(benzene)-type molecules **11** and **12**.[15]

The combined distortions have a striking effect on the metal–metal distance. In **4** and **5** it is ca. 0.48 and 0.44 Å longer than that calculated for an idealized geometry.

Electrochemical Studies. The cyclic voltammograms (CV) of the dinuclear compounds **4** (Figure 3A) and **5** dissolved in propionitrile showed two well-separated oxidations. In THF the resolution of the consecutive waves was less good but sufficient to show that in the trinuclear

(8) Haaland, A. *Top. Curr. Chem.* **1975**, *53*, 1.
(9) Elian, M.; Chen, M. M. L.; Mingos, D. M. P.; Hoffmann, R. *Inorg. Chem.* **1976**, *15*, 1148.
(10) The definition of the fold angle in **4** and **5** is slightly different from that of the out-of-plane bending of a single substituent.
(11) (a) Struchkov, Yu, T.; Andrianov, V. G.; Sal'nikova, T. N.; Lyatifov, I. R.; Materikova, R. B. *J. Organomet. Chem.* **1978**, *145*, 213. (b) Freyberg, D. P.; Robbins, J. L.; Raymond, K. N.; Smart, J. C. *J. Am. Chem. Soc.* **1979**, *101*, 892.
(12) Mues, P.; Benn, R.; Krüger, C.; Tsay, Y.-H.; Vogel, E.; Wilke, G. *Angew. Chem.* **1982**, *94*, 879; *Angew. Chem., Int. Ed. Engl.* **1982**, *21*, 868; *Angew. Chem. Suppl.* **1982**, 1891.
(13) Scroggins, W. T.; Rettig, M. F.; Wing, R. M. *Inorg. Chem.* **1976**, *15*, 1381.
(14) Paquette, L. A.; Schirch, P. F. T.; Hathaway, S. I.; Hsu, L.-Y.; Gallucci, J. C. *Organometallics* **1986**, *5*, 490.
(15) Traylor, T. G.; Goldberg, M. J.; Miksztal, A. R.; Strouse, C. E. *Organometallics* **1989**, *8*, 1101.

compound **6** every ferrocene unit is oxidized at a different potential (Figure 3B). The precision of the data collected in Table IV is therefore higher in PrCN (±5 mV) than in THF (±10 mV), and the separation of the second and the third potential of **6**, $\Delta E_{1/2}(3-2)$, should be regarded as an estimate. When ferrocene was investigated under similar conditions, the distance between the oxidation and reduction peak, ΔE_p, was in the range established by the ΔE_p values in Table IV for both solvents. Thus, the oxidations of **4**–**6** are similarly reversible as that of ferrocene.[16]

The first oxidation of **4** and **5** in THF occurs 160–170 mV more cathodic than that of Cp_2Fe.[17] This must be ascribed mainly to the fact that **4** and **5** are doubly alkylated ferrocenes and that increasing alkylation of Cp ligands facilitates the electron transfer.[18] The $E_{1/2}$ shift caused by one bridging substituent per ferrocene amounts to 135–170 mV to lower potential. If this is applied to **6**, $E_{1/2}(1)$ = 300 mV is in reasonable agreement with two bridges per ferrocene and the first electron transfer of **6** is therefore assigned to the central ferrocene unit. There seems to exist a "steric" contribution to the cathodic shift of $E_{1/2}$ because the isomers **4** and **5** are oxidized at different potentials (at least) in PrCN. $E_{1/2}(2)$ of **4** and **5** is close to $E_{1/2}$ of Cp_2Fe, which means that the electron-withdrawing effect of the fragment $CpFe^+$[19] roughly cancels the electron-donating effect of the alkyl bridge.

Dinuclear ferrocenes have long been known to show separate oxidation potentials.[20] It is generally accepted that the separation of the potentials, $\Delta E_{1/2}$, is a measure of the interaction between the ferrocene units. Since the electron is removed from an orbital that is essentially metal in character, $\Delta E_{1/2}$ is actually a measure of the metal–metal interaction. The main contribution to $\Delta E_{1/2}$ should be the electrostatic interaction, which is confirmed by the CV of **6**. Here the second wave corresponds to the oxidation of the first outer ferrocene unit; its spacing from the first wave, $\Delta E_{1/2}(2-1)$, is large because it is due to the charge on the central ferrocene which is only about 6.1 Å apart (cf. X-ray results of **4**). For the oxidation of the second outer ferrocene there should be no third wave in the CV if only the central charge were responsible for $\Delta E_{1/2}$. $\Delta E_{1/2}(3-2)$ may therefore be ascribed to the charge on the outer ferrocene; it is small because the charge is about 12.2 Å away.

Although the Fe–Fe distances in **4** and **5** differ by almost 0.8 Å, $\Delta E_{1/2}(2-1)$ values are equal within the experimental error. This could be explained by the limited resolution of the CV method. However, the electrostatic model is too simple; we also have to consider electronic delocalization and superexchange, which may be responsible for the greater $\Delta E_{1/2}(2-1)$ value of **6**. Further studies to clarify this question are in progress.

Conclusion

Our results open a general access to stereochemically well-defined oligonuclear metallocenes in which the neighboring sandwich units include angles of about 88 and 57° depending on the arrangement, syn,syn or syn,anti. The latter is associated with some selectivity in the formation of the compounds: The isomer ratio of the dinuclear derivatives suggests that in the dianion **3** the Cp faces with a neighboring ethano bridge are preferred for binding a CpFe unit. The selectivity may be related to the fact that cyclopentadienyllithium species are susceptible to the formation of triple ions.[21] When the metal–metal interaction is probed by cyclic voltammetry, its dependence on the inter-metallocene angle is transformed to a dependence on the metal–metal distance. Cyclic voltammetry resolves different interactions in a trinuclear compound, but not in dinuclear compounds, even though severe distortions increase the difference of the metal–metal distance as compared to the idealized geometry.

Experimental Section

General Data. All manipulations with organolithium compounds and the chromatography of the iron compounds were carried out under an inert-gas atmosphere with use of Schlenk-tube techniques and dried, oxygen-free solvents.

Elemental analyses were performed by the microanalytical laboratory of the Anorganisch-chemisches Institut. Melting points were obtained from samples sealed in capillaries with a Büchi Model 150 melting point apparatus; no correction was applied. Solid-state IR spectra were recorded in KBr disks with a Perkin-Elmer Model 577 spectrometer. A Varian MAT 311A spectrometer was used for the electron impact (70 eV) mass spectra. Cyclic voltammograms were obtained under inert gas in home-made cells with a platinum-wire working electrode, a platinum-net or -plate counter electrode, and a saturated calomel electrode (SCE) or a Ag/AgCl/3 M KCl electrode. The electrochemical station consisted of either a Wenking ST 72 standard potentiostat, a Wenking VSG 72 voltage scan generator, and a Hewlett-Packard HP 7004B plotter or a Princeton Applied Research 173/276 potentiostat, an Epson RX-80 printer, a Hewlett-Packard HP 7090A plotter, and an Apple IIe computer. Solutions that were (5–10) × 10^{-4} M in the complex and 0.1 M in supporting electrolyte (n-Bu_4NPF_6) were prepared for the CV studies. The NMR spectra were recorded with a JOEL JNM GX 270 spectrometer at 310 K. Signal shifts are reported in ppm (δ values), taking the solvent signals (residual protons of deuterated solvents for ^1H) as internal standard: C_6D_6, δ(^1H) 7.15, δ(^{13}C) 128.0. The digital resolution was 0.37 and 0.49 Hz/point for ^1H and ^{13}C NMR spectra.

***syn,syn*-Bis(η⁵-cyclopentadienyl)(1,2,3,3a,8a-η⁵:4a,5,6,7,7a-η⁵-4,8-ethano-2,4,6,8-tetrahydro-*s*-indacene-2,6-diyl)diiron (4) and *syn,anti*-Bis(η⁵-cyclopentadienyl)-(1,2,3,3a,8a-η⁵:4a,5,6,7,7a-η⁵-4,8-ethano-2,4,6,8-tetrahydro-*s*-indacene-2,6-diyl)diiron (5).** The iron-containing reagent was prepared by adding 14 mL of a 1.04 M precooled (−78 °C) solution of CpNa (14.56 mmol) in THF to a slurry of 3.37 g (7.17 mmol) of $Fe_2Cl_4(THF)_3$ in 50 mL of THF at −78 °C. The resulting green solution was stirred for 30 min at −78 °C before further reaction.

To the 4,8-ethano-*s*-indacene derivative **1**[5] (1.27 g, 6.97 mmol) dissolved in a mixture of 60 mL of THF and 10 mL of TMEDA was added at −78 °C 10 mL of a 1.6 M solution of methyllithium in ether. The colorless solution immediately became yellow, and gas evolution was observed; when the reaction mixture was warmed to room temperature, the color changed to orange.

When the orange solution was cooled to −78 °C and added to the green iron-containing reagent, a brown mixture was obtained. This was warmed to room temperature and stirred for 2 days. The solvents were removed under vacuum, and the brown powder was extracted with 50-mL portions of pentane until the solution was colorless. After the solvent was stripped from the combined orange-red extracts, the remainder was transferred to a sublimation apparatus and most of the ferrocene (0.3 g) was removed at 50 °C and 10^{-2} Pa. From the remaining solid a saturated

(16) Gagné, R. R.; Koval, C. A.; Lisensky, G. C. *Inorg. Chem.* **1980**, *19*, 2854.

(17) Under the conditions applied for **4**–**6** Cp_2Fe gave 570 mV in THF vs SCE and 488 mV in PrCN vs Ag/AgCl/3 M KCl.

(18) (a) Hoh, G. L. K.; McEwen, W. E.; Kleinberg, J. *J. Am. Chem. Soc.* **1961**, *83*, 3949. (b) Little, W. F.; Reilley, C. N.; Johnson, J. D.; Sanders, A. P. *J. Am. Chem. Soc.* **1964**, *86*, 1382. (c) Hall, D. W.; Russell, C. D. *J. Am. Chem. Soc.* **1967**, *89*, 2316. (d) Sabbatini, M. M.; Cesarotti, E. *Inorg. Chim. Acta* **1977**, *24*, L9.

(19) (a) Bowyer, W. J.; Geiger, W. E.; Boekelheide, V. *Organometallics* **1984**, *3*, 1079. (b) Desbois, M.-H.; Astruc, D. *Organometallics* **1989**, *8*, 1841.

(20) Gorton, J. E.; Lentzner, H. L.; Watts, W. E. *Tetrahedron* **1971**, *27*, 4353.

(21) Paquette, L. A.; Bauer, W.; Sivik, M. R.; Bühl, M.; Schleyer, P. v. R. *J. Am. Chem. Soc.*, in press.

Table V. Crystal Structure Data for 4 and 5

	4	5
cryst dimens, mm	0.4 × 0.3 × 0.1	0.15 × 0.20 × 0.55
formula	$C_{24}H_{22}Fe_2$	$C_{24}H_{22}Fe_2 \cdot 0.5C_6H_6$
M_r	422.133	461.194
cryst syst	monoclinic	monoclinic
space group	$P2_1/n$ (No. 14)	$P2_1/n$ (No. 14)
a, Å	8.665 (1)	6.087 (1)
b, Å	7.724 (1)	41. 475 (4)
c, Å	26.286 (2)	7.995 (1)
β, deg	97.82 (1)	96.58 (1)
V, Å^3	1742.9	2005.1
Z	4	4
d_{calcd}, g/cm^3	1.609	1.528
μ(Mo Kα), cm^{-1}	16.7	14.6
F(000), e	872	956
T, °C	22	22
$[(\sin \vartheta)/\lambda]_{max}$, Å^{-1}	0.639	0.593
hkl range	+12,+9,±35	+7,+49,±9
scan	ω	ω
scan width, deg in ω	0.85 + 0.35 tan ϑ	1.0 + 0.35 tan ϑ
no. of rflns measd	4294	3940
no. of unique rflns	3767	3518
R_{int}	0.01	0.04
no. of reflns obsd $[F_o \geq 4.0\sigma(F_o)]$	3107	2219
param ref	235	262
R^a	0.029	0.080
$R_w{}^b$	0.028	0.074
(shift/error)$_{max}$	0.007	0.05
$\Delta\rho_{fin}$ (max/min), e/Å^3	+0.31/−0.39	+0.89/−0.59

$^a R = \sum(||F_o| - |F_c||)/\sum|F_o|$. $^b R_w = [\sum w(|F_o| - |F_c|)^2/\sum F_o^2]^{1/2}$. $w = 1/\sigma^2(F_o)$. Function minimized: $\sum w(|F_o| - |F_c|)^2$ (SHELX-76).

pentane solution was prepared and chromatographed on silica. Two bands (I, II) were eluted with pentane, band III was eluted with pentane/toluene (3/1), band IV with toluene, and band V with ether. Band V gave a few milligrams of a red oil, which was not studied further. Bands II–IV were each chromatographed a second time as described.

Band I gave 0.1 g of ferrocene.

Band II gave orange crystals of **5** (0.81 g, 27.5% relative to **1**): mp 120 °C dec; IR (KBr) 3090 (m), 2950 (s), 2920 (s), 2840 (m), 1455 (w), 1430 (w), 1420 (w), 1410 (w), 1385 (w), 1362 (w), 1305 (w), 1290 (w), 1272 (w), 1200 (w), 1175 (w), 1132 (w), 1120 (w), 1100 (s), 1050 (w), 1030 (w), 1020 (w), 1015 (w), 997 (s), 885 (w), 875 (w), 830 (w), 815 (s), 805 (m), 705 (m), 630 (w), 565 (w), 480 (s), 455 (s), 345 (w), 325 (w) cm^{-1}; MS m/z (%) 424 (5, $M^+ + 2$), 423 (31, $M^+ + 1$), 422 (100, M^+), 421 (4, $M^+ - 1$), 420 (13, $M^+ - 2$), 396 (3, $M^+ + 2 - C_2H_4$), 395 (20, $M^+ + 1 - C_2H_4$), 394 (69, $M^+ - C_2H_4$), 393 (10, $M^+ - 1 - C_2H_4$), 392 (25, $M^+ - 2 - C_2H_4$), 329 (4, $M^+ - C_2H_4 - Cp$), 273 (33, $M^+ - C_2H_4 - CpFe$), 211 (9, M^{2+}), 152 (18, $M^+ - C_2H_4 - 2CpFe$), 121 (45, $CpFe^+$). Anal. Calcd for $C_{24}H_{22}Fe_2$: C, 68.29; H, 5.25; Fe, 26.46. Found: C, 68.89; H, 5.37; Fe, 26.22.

Band III gave orange crystals of **4** (1.02 g, 34.7% relative to **1**): mp 230 °C dec; IR (KBr) 3060 (w), 2950 (sh), 2920 (s), 2840 (m), 1450 (m), 1260 (w), 1130 (w), 1120 (w), 1105 (s), 1020 (m), 1000 (s), 880 (w), 840 (m) 815 (s), 690 (w), 540 (w), 485 (w), 480 (w), 465 (s) cm^{-1}; MS m/z (%) 424 (5, $M^+ + 2$), 423 (30, $M^+ + 1$), 422 (100, M^+), 421 (4, $M^+ - 1$), 420 (13, $M^+ - 2$), 396 (2, $M^+ + 2 - C_2H_4$), 395 (5, $M^+ + 1 - C_2H_4$), 394 (3, $M^+ - C_2H_4$), 393 (6, $M^+ - 1 - C_2H_4$), 329 (2, $M^+ - C_2H_4 - Cp$), 273 (12, $M^+ - C_2H_4 - CpFe$), 211 (17, M^{2+}), 152 (8, $M^+ - C_2H_4 - 2FeCp$), 121 (14, $CpFe^+$). Anal. Calcd for $C_{24}H_{22}Fe_2$: C, 68.29; H, 5.25; Fe, 26.46. Found: C, 68.65, 68.71; H, 5.61, 5.44.

Band IV gave 50 mg of an orange powder that, according to NMR and mass spectroscopy, was **6** containing a small amount of a nonvolatile saturated hydrocarbon: MS m/z (%) 661 (2, $M^+ + 3$), 660 (12, $M^+ + 2$), 659 (48, $M^+ + 1$), 658 (100, M^+), 657 (9, $M^+ - 1$), 656 (19, $M^+ - 2$), 630 (2, $M^+ - C_2H_4$), 602 (0.2, $M^+ - 2C_2H_4$), 329 (20, M^{2+}), 273 (16, $M^+ - C_2H_4 - Fe(C_{14}H_{12})FeCp$), 121 (13, $CpFe^+$).

X-ray Structure Determinations. Suitable single crystals of **4** and **5** were obtained by slowly evaporating benzene solutions. They were sealed under argon at dry-ice temperature into glass capillaries and examined directly on the diffractometer (Enraf-Nonius CAD4, Mo Kα radiation, λ = 0.710 69 Å, graphite monochromator).

Exact cell constants were determined by least-squares refinement on the Bragg angles of 25 centered reflections. Reduced cell calculations did not indicate Laue symmetry higher than monoclinic. Table V contains the crystal data as well as prominent numbers pertinent to data collection and structure refinement.

Both structures were solved by standard Patterson techniques. The crystals of **5** contained $^1/_2$ equiv of interstitial benzene per formula unit. It is situated around a crystallographic center of inversion and could be refined with anisotropic displacement

Table VI. Fractional Atomic Coordinates and Equivalent Isotropic Displacement Parameters^a for 4

atom	x/a	y/b	z/c	U_{eq}, Å^2
Fe1	0.3334 (1)	0.1440 (1)	0.0855 (1)	0.029
Fe2	0.9350 (1)	0.5037 (1)	0.1775 (1)	0.027
C1	0.7145 (3)	0.2169 (3)	0.1034 (1)	0.028
C2	0.5641 (3)	0.1484 (3)	0.1194 (1)	0.026
C3	0.4779 (3)	0.2737 (3)	0.1432 (1)	0.027
C4	0.5549 (3)	0.4505 (3)	0.1493 (1)	0.029
C5	0.7127 (3)	0.4081 (3)	0.1790 (1)	0.027
C6	0.7998 (3)	0.2864 (3)	0.1539 (1)	0.025
C7	0.6722 (3)	0.3740 (3)	0.0679 (1)	0.035
C8	0.5834 (3)	0.5122 (3)	0.0952 (1)	0.035
C9	0.4956 (3)	−0.0165 (3)	0.1249 (1)	0.033
C10	0.3636 (3)	0.0088 (4)	0.1517 (1)	0.036
C11	0.3533 (3)	0.1887 (4)	0.1633 (1)	0.033
C12	0.7910 (3)	0.4336 (3)	0.2296 (1)	0.034
C13	0.9288 (3)	0.3289 (4)	0.2347 (1)	0.036
C14	0.9350 (3)	0.2367 (3)	0.1878 (1)	0.032
C15	1.1249 (3)	0.5799 (3)	0.1439 (1)	0.039
C16	0.9886 (3)	0.6601 (4)	0.1190 (1)	0.039
C17	0.9226 (3)	0.7591 (3)	0.1557 (1)	0.042
C18	1.0185 (3)	0.7394 (3)	0.2035 (1)	0.041
C19	1.1421 (3)	0.6297 (4)	0.1963 (1)	0.037
C20	0.2453 (5)	0.0109 (6)	0.0211 (1)	0.057
C21	0.1268 (4)	0.0480 (5)	0.0497 (1)	0.048
C22	0.1167 (3)	0.2261 (5)	0.0541 (1)	0.047
C23	0.2278 (4)	0.3025 (5)	0.0290 (1)	0.051
C24	0.3112 (4)	0.1717 (8)	0.0077 (1)	0.055

$^a U_{eq} = (U_1U_2U_2)^{1/3}$, where U_i's are the eigenvalues of the U_{ij} matrix.

Table VII. Fractional Atomic Coordinates and Equivalent Isotropic Displacement Parameters for 5

atom	x/a	y/b	z/c	U_{eq}, Å^2
Fe1	0.1021 (3)	0.0856 (1)	0.1262 (2)	0.032
Fe2	−0.1915 (3)	0.1890 (1)	−0.2298 (2)	0.027
C1	−0.2769 (17)	0.1425 (2)	0.0903 (12)	0.024
C2	−0.1119 (19)	0.1211 (2)	0.1886 (12)	0.029
C3	0.1107 (18)	0.1331 (2)	0.2016 (12)	0.025
C4	0.1314 (17)	0.1655 (2)	0.1145 (13)	0.022
C5	0.0204 (18)	0.1610 (2)	−0.0632 (12)	0.024
C6	−0.1997 (19)	0.1483 (2)	−0.0750 (12)	0.021
C7	−0.2645 (18)	0.1751 (2)	0.1915 (12)	0.029
C8	−0.0141 (18)	0.1876 (2)	0.2088 (12)	0.029
C9	−0.1175 (20)	0.0940 (3)	0.2992 (13)	0.038
C10	0.1078 (19)	0.0896 (3)	0.3797 (11)	0.026
C11	0.2368 (19)	0.1139 (3)	0.3189 (13)	0.037
C12	0.0875 (20)	0.1612 (2)	−0.2295 (13)	0.032
C13	−0.0883 (22)	0.1487 (2)	−0.3437 (12)	0.031
C14	−0.2669 (21)	0.1408 (2)	−0.2489 (13)	0.032
C15	−0.2554 (22)	0.2340 (3)	−0.1377 (13)	0.036
C16	−0.4507 (22)	0.2193 (2)	−0.2010 (13)	0.032
C17	−0.4422 (22)	0.2130 (2)	−0.3767 (15)	0.038
C18	−0.2296 (22)	0.2235 (3)	−0.4163 (13)	0.037
C19	−0.1218 (22)	0.2369 (2)	−0.2654 (16)	0.035
C20	0.0093 (29)	0.0694 (3)	−0.1091 (17)	0.054
C21	0.0044 (27)	0.0445 (3)	0.0012 (18)	0.050
C22	0.2179 (36)	0.0403 (3)	0.0855 (17)	0.053
C23	0.3493 (25)	0.0638 (4)	0.0134 (21)	0.058
C24	0.2173 (30)	0.0816 (3)	−0.1046 (15)	0.048
C25	0.3566 (59)	0.0108 (8)	0.6126 (27)	0.078
C26	0.5489 (71)	0.0268 (4)	0.5933 (44)	0.081
C27	0.3073 (33)	−0.0163 (8)	0.5124 (51)	0.079

parameters. Relatively large values for the latter indicated some positional disorder and/or appreciable thermal movement. A nonlinear decay of -22.6% of the reflection intensities of **5** during the data collection might have been caused by loss of interstitial benzene and could have contributed as well to the large displacement parameters. The decay was corrected for isotropically on the basis of the intensity variation of three mutually orthogonal standard reflections. A decay of -0.7% for **4** was not corrected for. Due to the platelike single crystals of **4** an empirical absorption correction was necessary, which was based on scans around the diffraction vectors of nine selected reflections near $\chi = 90°$ (relative transmission 0.72-1.00).

For **4** all hydrogen atoms could be located in difference syntheses after the anisotropic refinement of the non-H atoms. For **5** only five hydrogen atoms could be located; the remainder were calculated at idealized geometrical positions. The benzene hydrogen atoms were neglected. For both structures the H atoms were included as fixed-atom contributions in structure factor calculations, while all other atoms were refined anisotropically. Tables VI and VII contain the atomic coordinates of the non-H atoms.

Acknowledgment. We thank J. Riede for collecting the X-ray data sets, Drs. J. Blümel and N. Hertkorn for some NMR spectra, and Dr. Ch. Habarta for assistance in the CV work. We also thank the Deutsche Forschungsgemeinschaft, the Fonds der Chemischen Industrie, and BASF AG for support.

Supplementary Material Available: Complete tables of hydrogen atom parameters and thermal parameters for **4** and **5** (6 pages); listings of observed and calculated structure factors (31 pages). Ordering information is given on any current masthead page.

Chemistry of Metal Oxo Alkyl Complexes. Mechanistic Studies on the Anaerobic and Aerobic Decompositions of Molybdenum(VI) Dioxo Dialkyl Complexes

William M. Vetter and Ayusman Sen*

Chandlee Laboratory, Department of Chemistry, The Pennsylvania State University, University Park, Pennsylvania 16802

Received July 10, 1990

The anaerobic and aerobic decompositions of $L_2Mo(O)_2R_2$ [L_2 = 4,4'-dimethyl-2,2'-dipyridyl, R = CH_2Ph, **1**; R = $CH_2C_6H_4CH_3$-*p*, **2**; R = $(CH_2)_4CH{:}CH_2$, **3**; R = CH_2CHMe_2, **4**; R = CH_2CMe_3, **5**; R = CH_2CMe_2Ph, **6**] were studied. The anaerobic decomposition mode chosen by a given $L_2Mo(O)_2R_2$ complex is a sensitive function of the hydrocarbyl group, R. If accessible β-hydrogens are present on R (as in **3** and **4**), equal amounts of alkane and alkene are formed through a β-hydrogen abstraction pathway. In the case of **4**, an additional pathway involving Mo-R bond homolysis accounts for 10% of the products formed. When β-hydrogens are absent from R (as in **1**, **2**, and **6**), the free radical, R$^\bullet$, formed by Mo-R bond homolysis is the predominant product. However, in every case there is an additional minor pathway for the formation of the alkane, RH, that involves α-hydrogen abstraction from the neighboring hydrocarbyl group. Because of the expected low stability of the primary neopentyl radical, the α-hydrogen abstraction pathway, rather than Mo-R bond homolysis, predominates in the decomposition of **5**. The reaction of the $L_2Mo(O)_2R_2$ complexes with O_2 appears to proceed almost exclusively through the intermediacy of the free radical, R$^\bullet$. In inert solvents, the principal organic product is the corresponding aldehyde, and the role of O_2 in its formation from $L_2Mo(O)_2R_2$ is 2-fold: (a) O_2 promotes the homolysis of the Mo-R bond to form R$^\bullet$, and (b) O_2 traps the resultant radical to yield the aldehyde. Labeling studies indicated that O_2, rather than the Mo=O group, was the predominant source of oxygen for the aldehydes. Mechanistic implications of our observations for the heterogeneous oxidation of alkanes and alkenes by Mo(VI)- and V(V)-oxo species are discussed.

MoO_3 and V_2O_5, either alone or in combination with other acidic oxides, catalyze a number of selective oxidations of alkenes and alkanes.[1] Many of these are of commercial interest, such as the oxidation of propylene to acrolein (eq 1) for the remarkable conversion of butane to maleic anhydride (eq 2). A salient feature of these processes is the rate-limiting direct interaction of the substrate with the metal-oxo species.[1a,d,e] For propylene oxidation, the initial formation of a symmetrical allyl intermediate has been established.[2] Moreover, experiments with $^{18}O_2$ and ^{18}O-labeled catalysts have revealed that the source of oxygen for acrolein is adsorbed or free O_2 at lower reaction temperatures and the metal-oxo group at higher temperatures.[3] Thus, the general features of these oxidations indicate that an intermediate alkyl (or allyl) species is formed initially and that this is followed by oxygen transfer from either O_2 or a metal-oxo species. In order to gain a detailed understanding of the latter step, i.e., the conversion of the metal-bound hydrocarbyl group to the corresponding oxidized organic products, we have initiated an examination of the chemistry of Mo(VI) oxo alkyl complexes.[4] As detailed blow, our results allow us to

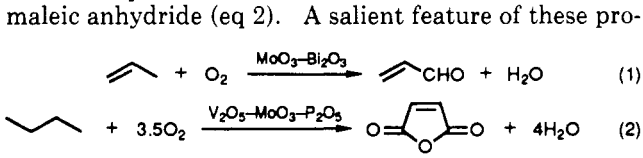

(1) Reviews: (a) Centi, G.; Trifiro, F.; Ebner, J. R.; Franchetti, V. M. *Chem. Rev.* **1988**, *88*, 55. (b) Hodnett, B. K. *Catal. Rev.-Sci. Eng.* **1985**, *27*, 373. (c) Cullis, C. F.; Hucknall, D. J. *Catalysis* **1982**, *5*, 273. (d) Keulks, G. W.; Krenzke, L. D.; Notermann, T. M. *Adv. Catal.* **1978**, *27*, 183. (e) Sheldon, R. A.; Kochi, J. K. *Metal Catalyzed Oxidations of Organic Compounds*; Academic: New York, 1981; Chapter 6.

(2) (a) Adams, C. R.; Jennings, T. J. *J. Catal.* **1964**, *3*, 549; **1963**, *2*, 63. (b) McCain, C. C.; Gough, G.; Godin, G. W. *Nature* **1963**, *198*, 989.

(3) Sancier, K. M.; Wentrcek, P. R.; Wise, H. *J. Catal.* **1975**, *39*, 141.

0276-7333/91/2310-0244$02.50/0